euspen's 21st International Conference & Exhibition, Copenhagen, DK, June 2021
www.euspen.eu

Effect of powder particle size on the rheology of feedstocks for low pressure powder injection moulding

Alberto Basso [1], Yang Zhang [1], Gamze Yilan[1], Jon Spangenberg [1], Hans Nørgaard Hansens[1]

[1]*Technical University of Denmark, Department of Mechanical Engineering, Kgs. Lyngby, Denmark*

albass@mek.dtu.dk

Abstract
Powder Injection Moulding (PIM) is a widespread technology for the fabrication of metal and ceramic components. Thanks to recent development within the field of Additive Manufacturing (AM), more and more focus is spent on the integration between AM and PIM. The use of AM to produce moulds for the injection moulding sector has pointed out new challenges: among others, the mould deformation during the filling stage. This issue is particularly severe when dealing with the injection of PIM feedstocks. The high viscosity of PIM feedstocks require elevated injection pressures. In this paper, the possibility to tailor the rheological properties of a feedstock by changing the distribution of powder particle size is investigated, taking into consideration the effect of specific surface area and interparticle forces. Finer powders with narrower distribution, higher specific surface area and presence of colloids showed higher viscosity, while coarse powder with broader particle size distribution and mainly non-colloidal particles resulted in lower viscosity.

PIM, AM, Soft Tooling, Powder Particle Size Distribution, Freeform Injection Moulding, Rheology, Low Pressure.

1. Introduction

Powder Injection moulding (PIM) is an established process for large-scale production of near net shape parts. This technology differs from conventional injection moulding (IM) due to the nature of the injected material: while in IM a polymer is injected into a mould, in PIM, metal or ceramic powders suspended in a polymer are instead used. Additive manufacturing (AM) has opened new horizons for PIM. The use of 3D printed moulds, instead of the milled metal tools, has enabled new design possibilities, overcoming some limitations of the conventional injection moulding process [1]. In case of highly customized parts, complex geometries are often needed, and a low overall number of parts produced. In such a situation, traditional PIM processes fail to comply since fabrication of moulds for intricate parts can be both challenging and expensive. The use of additive manufactured moulds as tools for injection moulding, called soft tooling, is a promising and affordable approach to use for PIM processes also when few parts are produced [2]. Another approach to soft tooling is the use of sacrificial moulds. This technique consents to produce components with complex geometry without the use of cores or slides as the mould is removed either thermally [3] or chemically [4].

Although soft tooling has allowed fabrication of customized parts, it creates a new set of interesting challenges for researchers and industry. Moulds for soft tooling are usually produced either by Fused Filament Fabrication as showed by Qayyum et al. [5] or by Vat Photopolymerization as described in a previous work of the authors [6]. These moulds are made of polymeric materials and not of metal, as the ones used in conventional IM. The strength of steel is up to four orders of magnitude higher than polymers and in particular photopolymers [7]. The pressure applied during the injection moulding process can create defects and deformations on the mould, due to the lower stiffness of the polymeric materials. Davoudinejad et al. [8], showed how an elevated packing pressure can cause damage when soft tools are used. Similar results are also observed by Zhang et al. [9]. It is impelling to avoid such defects in order to produce precise parts. The lower strength of the moulds is a particular challenge when dealing with PIM processes. The feedstock for PIM has higher viscosity than common materials for injection moulding. Thus, it needs higher pressure during the filling phase [7]. In order to use low pressure to inject PIM feedstocks, Demeres et al. [10] have investigated the effect of different binders, showing low viscosity for binders based on Paraffin Wax (PW).

In addition, Aslan et al. [11] and Sotomayor et al. [12] investigated the effect of solid loading and particle size distribution, respectively on the rheology of feedstocks.

The effect of the distribution of the powder on the rheology can be challenging because it is influenced by several aspects: the width of the distribution (narrow or wide [13]), the shape (monodispersed or bimodal [14-15]), the specific surface area and the type of powder (colloidal particles or non-colloidal [16]).

This paper investigates the effect that the particle size distribution of 316L SS powders has on the rheology of PIM feedstocks focusing on the influence of the before mentioned characteristics. The final aim is to tailor the powder particle size distribution of the feedstock to reduce its viscosity and inject the material at lower pressure obtaining, in this way, geometrically stable parts.

2. Experimental procedure

PIM feedstocks generally consist of metallic or ceramic powders and a binder system. The feedstocks investigated in this work were composed of 316L stainless steel powders provided by Sandvik Osprey Ltd. and a binder system containing PW, low-density polyethylene (LDPE) and stearic acid (SA). PW was used

as the primary binder and it is responsible for the flowability of the material. LDPE was selected as the secondary binder, enabling the structural integrity of the part after the injection. LDPE was chosen in place of high-density polyethylene (HDPE) because it exhibits lower viscosity than HDPE, while still being able to provide sufficient strength to the material. Finally, SA was added as surfactant to assist powder dispersion. The powder binder ratio used was 70/30.

In order to investigate the effect of powder particle distribution on the viscosity of feedstocks, two types of 316L stainless steel powders, with d50 of 5 µm and 50 µm, respectively, were used and mixed in different ratios, as reported in table 1. The parameter d50, represents the value of particle size below which is possible to find the 50% of the distribution.

Table 1. Composition in percentage of volume of the different feedstocks.

Feedstock	316L SS d50=5µm	316L SS d50=50µm
0-100	0 %	100 %
25-75	25 %	75 %
50-50	50 %	50 %
75-25	75 %	25 %
100-0	100 %	0 %

The mixing was done using a magnetic mixer IKA C-MAG HS 7. Several parameters influence the mixing: time, speed, temperature, sequence of material addition etc. In order to make the mixing procedure repeatable, the mixing time was fixed at 30 minutes and the temperature was set at 120°C. Such a temperature was selected based on the injection temperature. Another important parameter is the sequence of material addition. To avoid agglomeration, initially only the binders were added, once they reached the liquid state, the powders, which had been previously mixed together in dry condition, were included gradually. Since the powders were progressively added, the viscosity of the mixture was changing constantly and the mixing speed needed to be adjusted accordingly.

The powder particle size distribution was measured using a Malvern Mastersizer 3000 in wet condition with deionized water as medium. This instrument measures the angular variation intensity of the scattered light generated when a laser beam hits a powder particle.

The rheological investigation was done using an Anton Paar modular compact rotational rheometer, using a parallel plate apparatus with a disk of 25 mm, and a gap between plate and disk of 0.7 mm. Frequency sweep tests were used to calculate the complex viscosity of the paste at frequencies from 0.1 to 100 HZ. This test allows to perform viscosity measurements in the non-destructive deformation range by oscillating a disk at a constant shear with varying frequency. In order to assure to be in the non-destructive deformation range, the selected constant shear needs to be inside the limit of the linear viscoelasticity region. Such a shear can be selected by previously running an amplitude sweep test, where the paste is oscillated at constant frequency while increasing the shear systematically. All the viscosity measurements were carried out at 120°C.

3. Results and Discussion

This section reports and discusses the results from the investigation of the rheology of the different feedstocks. First, the powder particle size distribution is described, and then the rheology measurements are reported.

3.1. Powder Particle Size Distribution

Ten samples for each feedstock were used to investigate the powder particle size distribution. In figure 1 and table 2, the results of this investigation are reported and summarized.

The feedstock 0-100 is the one with coarser powder, also visible by the low specific surface area (SSA) of only 26 m^2/Kg. From the micrograph of figure 1 (a), only big particles are visible.

Table 2. Powder particle size distribution and Specific Surface Area (SSA) of the five different feedstocks.

Feedstock	0-100	25-75	50-50	75-25	100-0
d10 [µm]	27.0	3.7	3.1	2.5	2.8
d50 [µm]	50.5	37.2	6.9	5.3	5.1
d90 [µm]	92.2	84.3	54.8	70.5	8.6
SSA [m^2/Kg]	26	120	196	264	345

This is in agreement with the analysis done on the distribution of the particles, where a d10 of 27 µm was found, meaning that only 10% of the particles have a size below 27 µm. From the curve of figure 1 (a), it is also possible to notice how there are no particles below 10 µm. Such a feedstock has a wide distribution spanning roughly from 10 to 200 µm.

By introducing 25% of stainless steel powder with a d50 of 5 µm (this is the case of feedstock 25-75) a bimodal distribution is observable, see figure 1 (b). A first peak lies below 10 µm and a second one is present at roughly 60 µm. The distribution of the particle does not start anymore at 10 µm; the presence of very small particles is depicted in the micrograph of figure 1 (b).

Feedstock 50-50 has an equal amount of 316L SS with d50=50 µm and d50=5 µm. The distribution of the powder is narrower in comparison to the previous ones, with particle sizes below 120 µm. Half of the particles of this feedstock have sizes smaller than 10 µm.

When the amount of fine powder in the feedstock is higher than the coarse one, such as for feedstock 75-25, the distribution becomes even narrower. Now the size of the particles is below 90 µm, and the second peak of the bimodal distribution is flattening out. Only few big particles are visible from the micrographs in figure 1 (d)

Finally, feedstock 100-0 is the one with the narrowest particle size distribution. In this case, 90% of the particles of the powders have a size below 10 µm. The curve in figure 1 (e) shows a unique peak around 5 µm, only small particles are visible from the micrograph.

Overall, it is possible to observe how, by increasing the amount of fine powder in the feedstock, the specific surface area increases, while the distribution of the size of the powders moves toward the left and becomes narrower.

3.2. Rheological Investigation

Figure 2 shows the variation of the complex viscosity at different angular frequencies. The feedstock with the lowest viscosity is 0-100 (i.e., the one with 100% 50 µm metal powder) while the paste showing the highest viscosity is the one with 100% 5 µm.

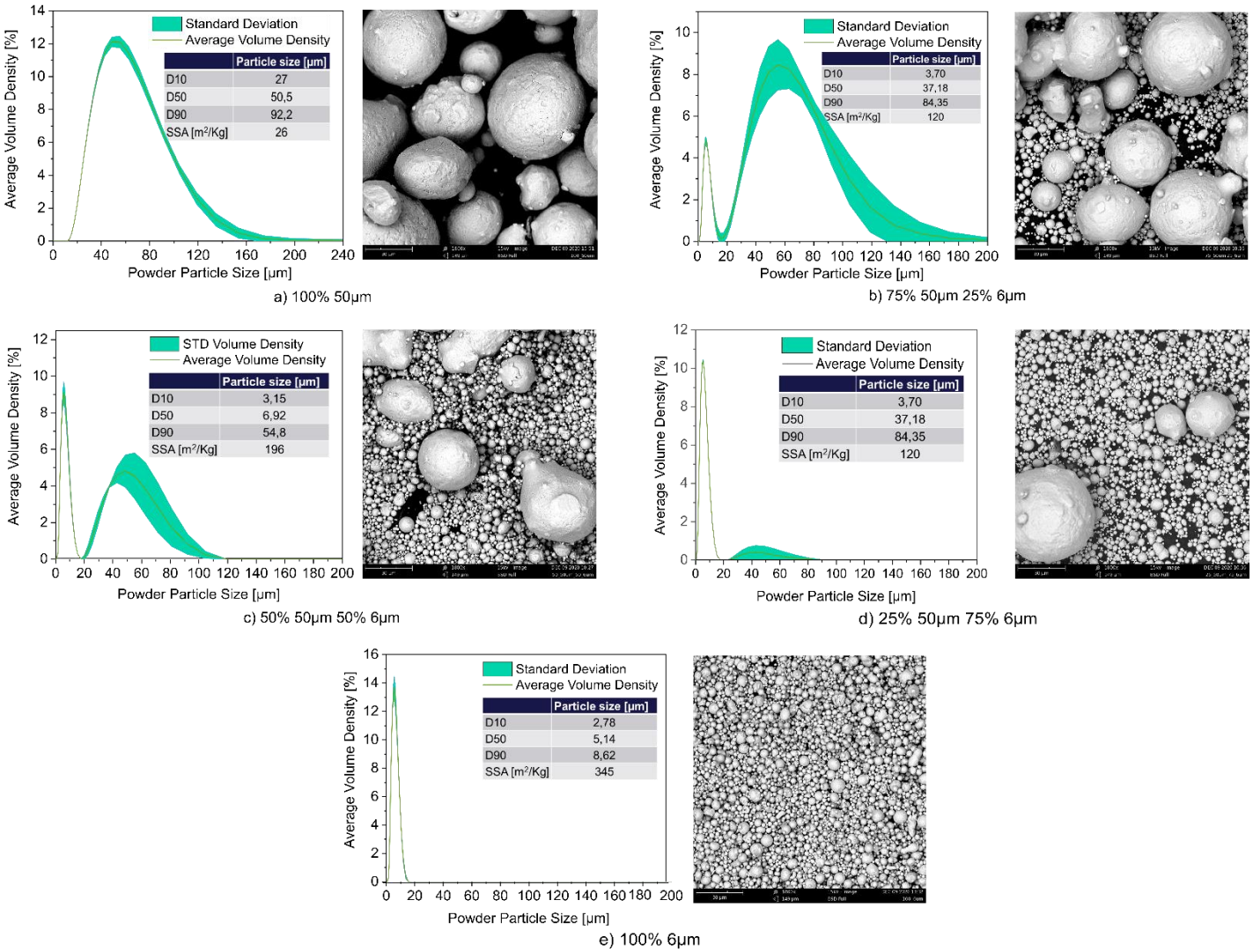

Figure 1. Powder particle size distribution of the five different feedstocks and related micrographs. The scale bar in the micrographs is 30 µm.

The viscosity of the feedstocks with a bimodal distribution are located in between the suspensions with monodispersed powders. This is also visible in figure 3, where the viscosities at small and large shear rate are reported. The result is in agreement with the one of Sotomayor et al. [12]. The straight curve with Newtonian behaviour at the bottom of figure 2 represents the viscosity of the binders system.

The discovery of the low viscosity of the feedstock with 100% 50 µm 316L SS powder, as compared to the other distributions, can be explained by considering the presence of both colloidal and non-colloidal particles in our feedstock. Genovese at al. [17] defined colloid, particles below 10 µm, and non-colloid, particles above 10 µm. Mehdipour et al. in [16] investigated the rheological properties of cementitious suspension and explained how, in the presence of non-colloidal particles, only mechanical interactions exist, and the viscosity is exclusively influenced by hydrodynamics and friction forces. In presence of colloidal particles instead, the rheology of the fluid is ruled by particle surface forces like Van der Waals and electrostatic interactions.

Colloids by definition have high specific surface area. The higher the specific surface area is, the more predominant the effect of the intermolecular forces over the hydrodynamics and friction forces. From the powder particle size investigation, we have seen that the addition of the fine powder with d50 of 5µm moves the distribution of the particle towards smaller size, thus increasing the amount of colloids in the feedstock.

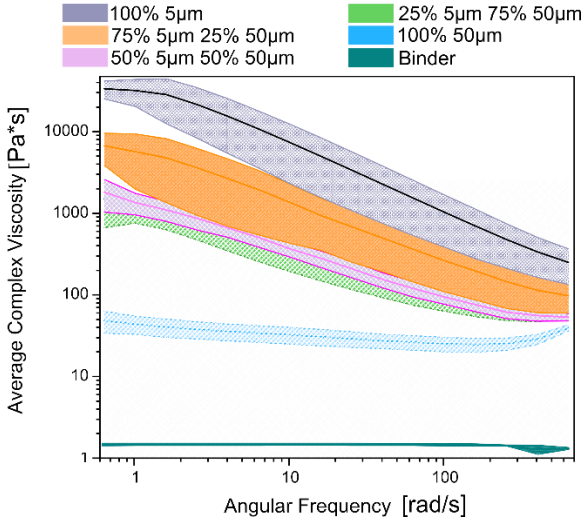

Figure 2. Average of the complex viscosity for the five different feedstocks and the binder. The coloured area around the curve depict the standard deviation.

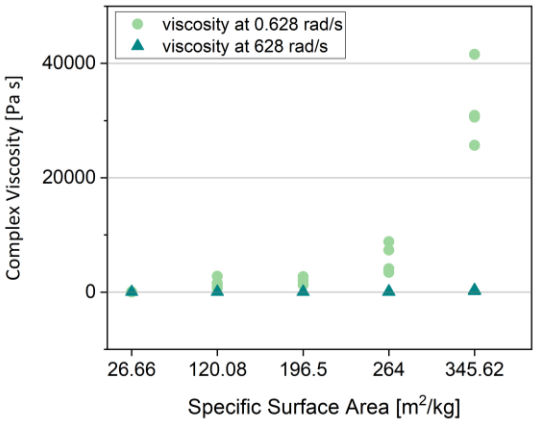

Figure 3. Complex viscosity for the five different feedstocks versus specific surface area. The viscosity data are reported for angular frequency of 0.628 rad/s and 628 rad/s.

An increase in colloids means that the particles in the suspension are closer to each other, increasing the interactions and thus the viscosity.

In Figures 3 and 4, it is possible to see the variation of the viscosity with specific surface area. Feedstock 100-0 (i.e., the one with 100% 5 µm metal powder) has the highest specific surface area, 345.62 m^2/Kg. In this case, the rheology is mainly influenced by the interactions forces, explaining the high viscosity of this feedstock. On the other hand, the feedstock 0-100 with 100% 50 µm powder has the lowest specific surface area and lowest viscosity.

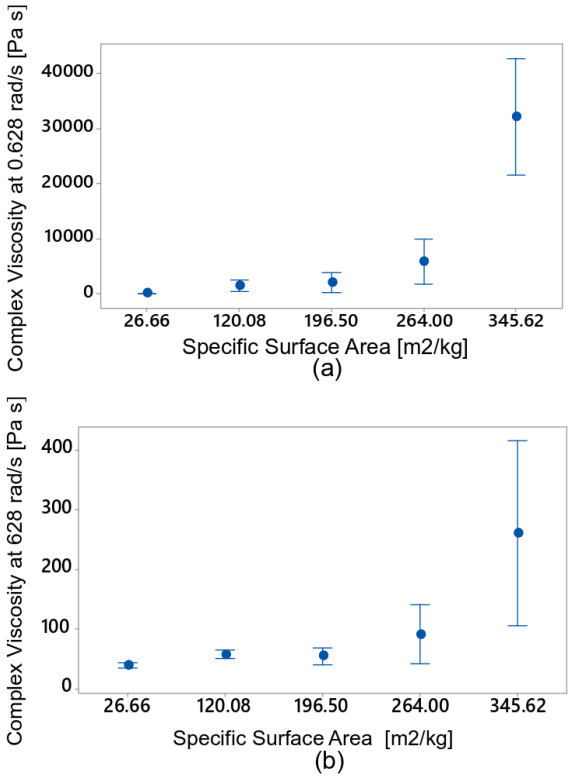

Figure 4. Interval plots of complex viscosity for the five different feedstocks versus specific surface area. The viscosity data are reported for angular frequency of 0.628 rad/s in (a) and 628 rad/s in (b).

It is possible to observe, in figure 3, how the deviation between the viscosity at low and high angular frequency increases with the increase of the specific surface area. Pseudo plastic fluids are characterized by a decrease in viscosity when the angular frequency is increased. The difference between the viscosity at low and high angular frequency for the feedstocks with smaller particle sizes, illustrates this pseudo plastic behaviour. The interval plot in figure 4, shows an increase of the standard deviation when the specific surface area is bigger. The increase in standard deviation is caused by a higher difference in viscosity of samples of the same feedstock. This behaviour might be caused by a higher tendency of the paste with finer powders to segregate.

Overall the feedstock with 100% 50 µm powder showed the lowest viscosity. This feedstock is a good candidate to reduce the pressure during injection moulding, however it might not reach the best densification during sintering due to the low specific surface area of its powder.

4. Conclusion

The aim of this paper was to investigate the effect of the powder particle size distribution. Five feedstocks with 70 % solid loading were produced using different ratio between two stainless steel powders with d50 of 5 µm and 50 µm.

The rheological investigation showed lower viscosity for the feedstock with 100% 50 µm 316L SS powder and higher viscosity for the suspension with bimodal distribution. The higher viscosity for the feedstock with a mix of powders can be explained by the presence of colloids promoting intermolecular forces over hydrodynamics and friction forces. A particular high viscosity was found for the feedstock with 100% 5 µm powder.

Considering that the paste with 100% 50µm powder showed both low viscosity and low standard deviation, it might be a good candidate as feedstock for low pressure injection moulding.

Acknowledgement

The work has been supported by Innovation Fund Denmark through the project "3DIMS – 3D-Printing Integrated Manufacturing System" (Grant no. 6151-00005A)

References

[1] Thompson M -K, Moroni G, Vaneker T, Fadel G, Campbell R. –I, Gibson, I Bernard, A. et al. 2016., *Annals of the CIRP* **65**/2: 737–60.
[2] Tosello G, Charalambis A, Kerbache L, Mischkot M, Bue Pedersen D, Caloan M and Nørgaard Hansen H. 2019 *The Int. J. of Advanced Manufacturing Technology*. **100** 783-795.
[3] Hein S. B, Otte A L. *2018 International Powder Metallurgy Congress and Exhibition*.
[4] Stampfl J, Wöß A, Seidler S, Fouad H, Pisaipan A, Shwager F and Liska R. 2004 *Macromol. Symp*. **217** 99-107
[5] Qayyum J A, Altaf K, Rani A M A, Ahmad F and Jahanzaib M. 2017, *ARPN Journal of Engineering and Applied Sciences*, **12**
[6] Basso A, Mendez Ribo M, Danielak A H, Yang B, Kjeldsteen P, Valler P, Zhang Y, 2019 *Joint Special Interest Group meeting between Euspen and ASPE Advancing Precision in Additive Manufacturing, Nantes, France.*
[7] Zhang Y, Basso A, Christensen S E, Bue Pedersen D, Staal L, Valler P and Nørgaard Hansen H. 2020. *Annals of the CIRP* **69**/1 185-188
[8] Davoudinejad A, Bayat M, Bue Pedersen D, Zhang Y, Hattel J H, and Tosello G. 2019. *The International Journal of Advanced Manufacturing Technology*. **102** 403-420.
[9] Zhang Y. Bue Pedersen D, Segebrecht Gøtje A and Mischkot M 2017 *J. of Manufacturing Processes.* **27** 138-144.
[10] Demeres V, Fareh F, Turenne S, Demarquette N R and Scalzo O. 2018. *Advanced Powder Technology*. **29** 180-190.
[11] Aslam M, Ahamad F, Yusoff P, Altaf K, Omar M A, Khalil A and Raza M R. 2016 *Advances in Materials Science and Engineering.*
[12] Sotomayor M E, Varez A, and Levenfeld B. 2010 *Powder Technology* **200** 30-36.
[13] Claudel D, Sahli M, Barreire T and Gelin JC. 2017 *Powder Technology*. **322** 273-289.
[14] Poslinski A J, Ryan M E, Gupta R K, Seshadry S G and Frechette F J 1988. *Journal of Rheology*, **32** 751-771
[15] Spangenberg J, Scherer G W, Hopkins A B and Torquato S. 2014. *Journal of Applied Physics.* **116.**
[16] Mehdipour I and Kayhat K H. 2018. *Construction and Building Materials.* **161** 340-353.
[17] Genovese D B, Lonzano J E and Rao M A. 2007. *Journal of Food Science*. **72.**